

# Characteristics of ZnO and Al Doped ZnO Thin Films Prepared by Sol Gel Method for Solar Cell Applications

**M.A. Bouacheria**

Université des Sciences et de la Technologie d'Oran Mohamed Boudiaf USTO-MB

**A. Djelloul** (✉ [djelloulcrtse@gmail.com](mailto:djelloulcrtse@gmail.com))

Research Center "CRTSE", Algiers, Algeria. <https://orcid.org/0000-0002-2226-1987>

**M. Adnane**

Université des Sciences et de la Technologie d'Oran Mohamed Boudiaf USTO-MB

---

## Research Article

**Keywords:** Zinc oxide, Al-doped ZnO, dip-coating technique, thin films, sol-gel, X-ray diffraction, photoluminescence

**Posted Date:** January 14th, 2022

**DOI:** <https://doi.org/10.21203/rs.3.rs-1243255/v1>

**License:**  This work is licensed under a Creative Commons Attribution 4.0 International License.

[Read Full License](#)

---

# Abstract

Pure and Al-doped ZnO (AZO) thin films with different aluminium (Al) concentrations (Al: 0.5, 1, 2, and 3 wt.%) were prepared on p-type Si(100) substrate by a dip-coating technique using different zinc and aluminum precursors. The structural, morphological, optical and electrical properties of these films were investigated using a number of techniques, including the X-Ray Diffraction (XRD), scanning electron microscopy (SEM), Atomic force electron microscopy (AFM), ultraviolet–visible spectrophotometry, photoluminescence(PL) spectroscopy and four-point probe technique. The X-ray diffraction (XRD) results shown that the obtained (AZO) films were polycrystalline with a highly c-axis preferred (002) orientation, and the average crystallites size decrease from 28.32 to 24.61 nm with the increase in Al dopant concentration. The studies demonstrated that the ZnO film had a good transparency in the visible range with the maximum transmittance of 95% and the band gaps ( $E_g$ ) varied from 3.16 to 3.26 eV by aluminum doping. Scanning electron microscopy (SEM) images showed that the surface morphology of the films changed with increase of Al-doping. The photoluminescence spectra also showed changed with Al-doping.

## 1. Introduction

Zinc oxide (ZnO) is an important and one of the most multifunctional semiconductor material used in different applications' domains like gas sensors [1], light emitting diodes (LED) [2], optoelectronic devices [3–5], window materials [6] and solar cells [7–10], owing to its direct wide band gap (3.37 eV) [11, 12] with a natural conductivity of type (n) and high exciton band energy (60 meV) at room temperature [13, 14].

Several physical and chemical deposition techniques were adopted to synthesize doped or un-doped zinc oxide films including, laser deposition [15, 16], sputtering [17], molecular beam epitaxy (MBE) [18], evaporation [19], chemical vapor deposition (CVD) [20], electrochemical deposition [21], spray pyrolysis [22–24], chemical bath deposition (CBD) [25, 26], successive ionic layer adsorption and reaction ( SILAR) [27], sol–gel method [28–30]. Among them, the Sol–gel (dip-coating) is a suitable method, because of its simple, low cost, efficient, easy control of doping, lower crystallization temperature and large-scale capability [31].

It has been reported that the doping of Zinc Oxide (ZnO) with various metal elements such as gallium (Ga), indium (In), Tin (Sn), Lead (Pb), Iron (Fe), Nickel (Ni) and aluminum (Al) improve some of its properties [32–38]. Among them, aluminum (Al) is commonly used to form Al-doped ZnO (AZO) to improve the conductivity of zinc oxide [39]. In the present work, undoped and Al- doped ZnO thin films were prepared by a dip-coating technique using different zinc and aluminum precursors and the effects of aluminum doping (concentration of Al: 0, 0.5, 1, 2, and 3 wt.%) on the structural, morphological, optical and electrical properties of ZnO thin films were examined.

## 2. Experimental Details

## 2.1. Sample Preparation:

The dip coating method was applied to deposit the undoped ZnO and Al-doped ZnO (AZO) thin films (Al: 0.5, 1, 2 and 3 at%) on both glass and p-type Si substrates of (100) plane. During the preparation of sol-gel, zinc acetate dehydrate  $\text{Zn}(\text{CH}_3\text{COO})_2 \cdot 2\text{H}_2\text{O}$  was used as the precursor material, ethanol ( $\text{C}_2\text{H}_6\text{O}$ ) as the solvent, monoethanolamine (MEA)  $\text{C}_2\text{H}_7\text{NO}$  as the sol stabilizer, and aluminium chloride hexahydrate ( $\text{AlCl}_3 \cdot 6\text{H}_2\text{O}$ ) as the dopant source.

The starting solution was prepared by 0.37 M of Zinc Acetate dissolved in 50 ml ethanol at room temperature and stirred for 15 minutes. After, heat was increased and maintain at  $60^\circ\text{C}$  for another 15 minutes. After that, MEA was added into the solution drop by drop in order to get the molar ratio of MEA and zinc was fixed at 1, and this is followed by aluminium chloride hexahydrate as the doping agent with various Al/Zn atomic ratios of Al; 0.5%, 1%, 2% and 3%. The temperature of the mixture was retained at  $60^\circ\text{C}$  and stirred for 2 hours. After a light yellowish clear and homogeneous solution was obtained, it was left at room temperature for 24 hours to allow aging process.

After conventional chemical cleaning of the substrates, the thin films were deposited on Si substrates by dip coating process, at the speed of 3 mm/s. The thin films were dried at  $300^\circ\text{C}$  in air for 10 min to remove the solvent and organic residuals. The cycle process of dip coating to drying was repeated 3 times (3 Cycles) to obtain multilayer films. At last, ZnO-Al thin films were annealed at  $500^\circ\text{C}$  in air ambient for 1 hour. A schematic drawn of the sol-gel dip coating process for the synthesis of the undoped and Al doped ZnO thin films is depicted in Fig. 1.

The structural, morphological, optical and electrical analysis of films has been investigated by XRD, AFM, SEM, UV spectroscopy, PL spectrophotometer and four-point probe technique were used to characterize the obtained ZnO thin films.

## 2.2. Characterization techniques:

The structure of the films is characterized by the PANalytical X'PERT Pro Philips diffractometer with a  $\text{CuK}\alpha$  radiation ( $\lambda = 1.54059 \text{ \AA}$ ). The film thickness was obtained by ellipsometry using SEMILAB Spectroscopic Ellipsometer. The morphology of the films was checked by scanning electron microscopy (SEM) JEOL JSM 6610 LA. The optical properties are determined by measuring the transmittance of the films using a spectrophotometer (Cary 500) in the wavelength range (300-1200) nm on glass substrates. The room temperature photoluminescence (PL) was performed using He-Cd laser as an excitation source operating at 325 nm. The PL spectra were recorded using HORIBA spectrometer iHR-550 equipped with CCD detector (400–1000 nm). Finally, the electrical properties (sheet resistance) of the films were measured using the four point probe conventional instrument.

## 3. Results And Discussion

### 3.1. X-ray diffraction (XRD) analysis:

Figure 2 shows the X-ray diffraction (XRD) patterns of undoped ZnO (Figure 2.a) and Al-doped ZnO thin film deposited on silicon substrates with concentration (Al: 3 wt. %) is presented on Figure 2.b. The XRD patterns shown in Fig. 2a exhibits several peaks located at 31.75°, 34.44°, 36.30°, 47.01°, 56.95° and 62.96°, corresponding to ZnO at orientations (100), (002), (101), (102), (110) and (103) respectively, with preferential orientation at (100). In addition, we observed that all peaks were in good agreement with the data base of standard ZnO (JCPDSN° 00-005-0664) with space group P63mc [40]. This analysis reveals the existence of a ZnO single-phase with a hexagonal wurtzite structure. The comparison of all XRD patterns of as prepared samples with the ASTM specifications ZnO confirmed that we have only the peaks of ZnO phase in the XRD spectrum. This result suggests that the deposited AZO films are polycrystalline with (002) as preferential orientation located around 34.40° (Fig. 2b). The intensity of the peak (002) increases proportionally with the concentration of Al up to achievement the maximum which is 3 wt% of Al. There is no extra peaks related to Al or secondary phase was observed before and after incorporation of (Al) in the ZnO thin films. This is due to difference in ionic radii of Zn<sup>2+</sup> (0.74 Å) and Al<sup>3+</sup> (0.54 Å) which it replaces their sites without changing the wurtzite structure of ZnO [41].

The lattice spacing of undoped and Al doped ZnO thin films were calculated using the Bragg's formula [42]:

$$2d_{hkl}\sin\theta = n\lambda$$

1

Where (h k l) are Miller indices;  $d_{hkl}$  is the lattice spacing;  $\theta$  is half of Bragg angle; and  $\lambda$  is the wavelength of the target XRD. Further, the lattice parameters (a,c) values calculated from the spectra obtained, determined from relation [43]:

$$\frac{1}{d_{hkl}^2} = \frac{h^2 + k^2}{a^2} + \frac{l^2}{c^2}$$

2

The average crystallite size was decreased with increasing Al doping concentration and calculated using the Debye– Scherrer's formula [32]:

$$D = \frac{K \cdot \lambda}{\beta \cos\theta}$$

3

Where: « D » is the crystallite size; «  $\lambda$  » is the wavelength of the incident X-rays used (1.54059Å); « k » is the Scherrer constant; «  $\beta$  » is the full width at half maximum (FWHM) of the diffraction peak and «  $\theta$  » is half of Bragg angle in degrees. The calculated structural parameters such as the position, FWHM, the lattice parameters "a" and "c", the grain size "D" and the average crystallite sizes are listed in Table 1.

**Table 1.** XRD parameters of ZnO undoped and Al-doped ZnO (Al: 3 wt. %).

Samples	(hkl)	2Theta (°)	FWHM(°)	a (Å)	c (Å)	D (nm)	Average D (nm)
ZnO	(100)	31,75337	0,3651	2,8157	5.2028	22,62	28,32
	(002)	34,44782	0,4003			20,77	
	(101)	36,30213	0,2011			41,57	
ZnO-Al: (3 wt. %)	(100)	31,31827	0,2787	2,8538	5.2027	29,60	24,61
	(002)	34,44822	0,4236			19,63	

As illustrated in Table 1, it was found that the grain size "D" of the undoped ZnO film is estimated to be 22.62, 20.77 and 41.57 nm according to the (100), (002) and (101) orientation while it is estimated to be 29.60 and 19.63 nm according to the (100) and (002) orientation of the Al doped ZnO thin films, respectively. Consequently, the average crystallite sizes of undoped and Al-doped ZnO (Al: 3 wt. %) were 28.32 nm and 24.61 nm, respectively [45–47]. Hence, the sharp peaks of the Al-doped ZnO (Al: 3 wt. %) film indicated high quality crystal growth, with relatively large crystallites according to the (002) orientation compared to that of undoped ZnO. Also, the values of lattice parameters (a, c) are distinctly show that for 3% Al the "c" parameter decrease while the "a" parameter increase, meaning the good insertion of Al atoms in the substitutional Zn sites, as mentioned above.

### 3.2. Atomic Force Microscopy (AFM) analysis :

Figure 3(a) and Figure 3(b) show typical 3D AFM images for 02 µm x 02 µm scanning of undoped ZnO and Al-doped ZnO (Al: 3 wt. %) semiconductor thin films deposited by dip coating method. It is observed that the Al-doping (Al: 3 wt. %) significantly affect the morphology and roughness of the ZnO films. The surface roughness (Arithmetic Average, Ra and Root Mean Square, Rq) increases from (Ra=1.1, Rq=1.3) to (Ra=2.13, Rq=2.68) with Al-doping concentration. This implies that the films have a smooth surface. It was also observed that the undoped ZnO film tend to form clusters.

It is worth noting that this lowers roughness and smoothness of the surface can assist transmit further light into absorber layer [48].

### 3.3. Scanning electron microscopy (SEM) analysis:

The morphology of undoped ZnO and doped with 0.2 and 3 wt.% of Al thin films was analysed by Scanning Electronique Microscope (SEM). From Fig. 4, one can see that the surfaces of all films exhibit a wrinkles-like morphology. The wrinkles-like formations are interconnected with each other, and do not have a particular orientation. Additionally, increasing the doping rate causes the morphological change of layers that affect the mechanisms of the nucleation and on wrinkles growth. Their length exceeds 10 µm. The wrinkles-like formations are thinner in the case of ZnO thin film doped with 3 wt% Al. This morphology is similar to that observed by other researchers [49]. Other scientific researchers have also suggested a link between the size of wrinkles and the percentage of dopants [50].

### 3.4. Optical (UV-vis-NIR) analysis :

Figure 5 shows the optical transmittance versus wavelength spectra of AZO films taken in the wavelength range, 350–1200 nm. As can be seen from Fig. 6, all the films were highly transparent in the visible range (400–700 nm) with a high transmittance. The undoped ZnO films showed an optical transmittance of > 70% while the Al-doped ZnO films with higher dopant concentration (> 1 at.% exhibited slightly high optical transmittance (> 85%) than films with lower doping concentration ( $\leq 1$  at.%) of aluminium. In the present study, the absence of interference peaks in the transmittance spectra might be attributed to low film thickness and small grain size of the grown films [51].

From transmittance measurements can be estimated by the optical band gap considering a direct gap semiconductor. The band gap ( $E_g$ ) was calculated by using the relation [52, 53]:

$$(\alpha h\nu)^2 = K (h\nu - E_g)$$

4

Where «  $h$  » is Planck's constant, «  $\nu$  » is the frequency of the incident radiation, «  $K$  » is a constant and  $E_g$  is the band gap energy. The absorption coefficient  $\alpha$  could be calculated using equation [54]:

$$\alpha = \frac{-\ln(T)}{d}$$

5

Where «  $T$  » is the transmittance and «  $d$  » is the thickness of the film.

Figure 6 shows the plots of  $(\alpha h\nu)^2$  against  $(h\nu)$  for the undoped and Al-doped ZnO thin films. The energy band gap ( $E_g$ ) of as prepared samples can be determined by extrapolating the linear part of the straight lines onto the energy axis to reach  $(\alpha h\nu) = 0$ . As can be seen from Fig. 6,  $E_g$  (pure ZnO) is equal to 3.09 eV. This value increased slightly with increasing Al doping concentration. The highest optical band gap, 3.26 eV, was achieved in the ZnO thin films doped with 3% Al [49]. The estimated optical band gaps are identical to those reported by several authors; this enables undoped and doped ZnO thin films to be a transparent material and justifies their use as front windows in optoelectronic devices [49, 50, 55].

### 3.5. Photoluminescence (PL) analysis:

The luminescence emission spectra are shown in Fig. 7 emitted from the samples of undoped and Al-doped ZnO (Al: 0.5, 1, 2 and 3 wt. %) thin films. Under the same conditions in range of 300 to 550 nm, all photoluminescence spectra were performed using He-Cd laser as an excitation source operating (325 nm) at room temperature. In this figure, it can be seen that there are different PL bands, including the Ultraviolet (UV) emission 377 nm, Violet-II emission 436 nm, Blue emission 473 nm and Green emission 518 nm. The intensity of UV emission at  $\sim 377$  nm increased as the Al doping increased up to 2 wt.% and then decreased at 3 wt.% Al. The high intensity of a green emission band at  $\sim 518$  nm was obtained in ZnO:Al (Al: 1, 2 and 3 wt. %) thin films as compared with that of undoped films. Nevertheless, the incorporation of aluminium in ZnO affects the photoluminescence significantly. Also, there are many

other emission bands corresponding to the visual field, mainly emanated from some defects such as Zinc interstitial and oxygen deficiency etc [45, 56–61].

## 3.6. Electrical Properties

The nature of the charge carriers were measured by the hot probe method. Pure and Al doped ZnO exhibits n-type conductivity. Fig. 5 shows the variation of electrical resistivity with different aluminium (Al) concentrations (Al: 0.5, 1, 2, and 3 wt.%). The resistivity decreases with increase in aluminium doping and varied from 54.61 to 04.592 M $\Omega$ /□. Increasing the concentration of aluminum leads to an increase in the amount of aluminum atoms and their incorporation into the ZnO thin films, leading to a decrease in sheet resistance [62]. AZO film with the concentration of (Al: 3 wt.%) showed excellent electrical and optical properties with the lowest sheet resistance of 4.59 M $\Omega$ /sq and highest values of the optical gap (3.26 eV) and transparency (> 85%), respectively.

## 4. Conclusion

The structural, morphological, optical and electrical properties of undoped ZnO and Al doped ZnO thin films deposited on glass substrates by dip-coating process were investigated. X-ray diffraction studies confirm that the films have polycrystalline nature with wurtzite hexagonal structure and preferred orientation along the (002) plane. The intensity of the peak (002) increases proportionally with the concentration of Al up to achievement the maximum which is 3 wt% of Al. The average crystallite size values of the films are found to be 28.32 and 24.61 nm for ZnO and AZO thin films, respectively. All deposited films have high transparency (70-95%) with absence of interference peaks in the transmittance spectra. The optical gap of our samples was found between 3.09 and 3.26 eV. This value increased slightly with increasing Al doping concentration. The highest optical band gap, 3.26 eV, was achieved in the ZnO thin films doped with 3% Al. PL studies show that all the films have near band emission. It also showed a strong ultraviolet and visible emission band which may be attributed to the aluminium doping leads to increase in oxygen vacancy and other defects such as Zinc interstitial etc. The AFM and SEM results indicates that the surface roughness increases from (Ra=1.1, Rq=1.3) to (Ra=2.13, Rq=2.68) with Al-doping concentration. Additionally, increasing the doping rate causes the morphological change of layers that affect the mechanisms of the nucleation and on wrinkles growth. Their length exceeds 10  $\mu$ m. The wrinkles-like formations are thinner in the case of ZnO thin film doped with 3 wt% Al. It was seen that the sheet resistance of ZnO thin films decrease with different aluminium (Al) concentrations (Al: 0.5, 1, 2, and 3 wt.%). These results indicate that, Al doped ZnO thin films were synthesized by low cost sol-gel dip coating technique can be considered as the promising candidate for solar cell applications.

## Declarations

## Acknowledgments

This work was supported by all members of Laboratory of Electron Microscopy and Materials Sciences, University of Science and Technology of Oran 'USTO'. The authors would like to thank Algerian Ministry

of Higher Education and Scientific Research and Directorate General for Scientific Research and Technological Development.

## Author Contributions

All authors contributed to the study conception and design. Material preparation, data collection and analysis were performed by Mohammed Amine Bouacheria, Abdelkader Djelloul and Mohamed Adnane. The first draft of the manuscript was written by Mohammed Amine Bouacheria and all authors commented on previous versions of the manuscript. All authors read and approved the final manuscript.

## Compliance with ethical standards

**Conflict of interest** The authors declare that they have no conflict of interest.

**Financial interests:** Funding financial support from the Directorate General for Scientific Research and Technological Development (Algerian Ministry of Higher Education and Scientific Research).

**Data Availability** Not applicable.

### Compliance with Ethical Standards

Conflict of Interest Not applicable.

Code Availability Not applicable.

Publisher's Note Springer Nature remains neutral with regard to jurisdictional claims in published maps and institutional affiliations.

## References

1. R. Viter, K. Kunene, P. Genys, D. Jevdokimovs, D. Erts, A. Sutka, K. Bisetty, A. Viksna, A. Ramanaviciene, A. Ramanavicius, Photoelectrochemical bisphenol S sensor based on ZnO-Nanoroads modified by molecularly imprinted Polypyrrole. *Macromol. Chem. Phys.* **221**, 1900232 (2020). <https://doi.org/10.1002/macp.201900232>
2. C.F. Liu, T.H. Chen, J.T. Huang, *Sens. Mater.* **32**, 3727 (2020). <https://doi.org/10.18494/SAM.2020.3>
3. A. Pricilla Jeyakumari, P. Siva, P. Pachamuthu, M. Revathi, *J. Appl. Phys.* **3**, 80–86 (2017)
4. A. Zaier, F. Oum El az, F. Lakfif, A. Kabir, S. Boudjadar, M.S. Aida, Effects of the substrate temperature and solution molarity on the structural opto-electric properties of ZnO thin films deposited by spray pyrolysis. *Mater. Sci. Semicond. Process.* **12**, 207–211 (2009). [doi:10.1016/j.mssp.2009.12.002](https://doi.org/10.1016/j.mssp.2009.12.002)
5. R. Koutavarapu, R.K.N.R. Manepalli, B.T.P. Madhav, M.C. Rao, J. Shim, Structural, optical and magnetic properties of Cd doped ZnO nanomaterials for optoelectronic device application. *J. Mater.*



- Sci.: Mater. Electron. **32**, 11264–11273 (2021). <https://doi.org/10.1007/s10854-021-05795-9>
6. B. Mereu, O. Caglar, J.S. Cashmore, P.A. Losio, A. Salabas, I. Sinicco “ Window p-layer in amorphous pin solar cells using ZnO as Transparent Conductive Oxide “. *Solar Energy Materials & Solar Cells* **152**, 147–154 (2016). <http://dx.doi.org/10.1016/j.solmat.2016.03.036>
  7. I.Y.Y. Bu, Novel all solution processed heterojunction using p-type cupric oxide and n-type zinc oxide nanowires for solar cell applications. *Ceram. Int.* **39**(7), 8073–8078 (2013)
  8. M. Melouki, H.F. Mehnane, A. Djelloul, Y. Larbah, M. Adnane. “Improvement of Electrical Properties of Grätzel Cells by Tuning the Dye Layer with CdS/ZnO Junction”. *J. Nano- Electron. Phys.* 13 No 4, 04004(5pp) (2021). DOI:10.21272/jnep.13(4).04004
  9. C. Tong, J.H. Yun, Y.J. Chen et al., Thermally diffused Al:ZnO thin films for broadband transparent conductor. *ACS Appl. Mater. Interfaces* **8**(6), 3985–3991 (2016)
  10. N. Hourri, A. Djelloul, M. Adnane. “Performance Comparison of Low Cost TiO<sub>2</sub> and ZnO Solar Cells Sensitized with Coumarin C343 “. *J. Nano- Electron. Phys.* 12 No 6, 06004(6pp) (2020). DOI:10.21272/jnep.12(6).06004
  11. A. Baltakesmez, S. Tekmen, S. Tuzemen, *J. Appl.Phys.* **110**, 054502–054507 (2011)
  12. M. Sahal, B.Hartiti,A. Ridah, M. Mollar, B. Mari, *Micr.elec.Jour.* **39**(12), 1425 (2008)
  13. D. Pellegrino, G. Franzò, V. Strano, S. Mirabella, E. Bruno, Improved Synthesis of ZnO Nanowalls: Effects of Chemical Bath Deposition Time and Annealing Temperature ». *Chemosensors* **7**, 18 (2019). doi:10.3390/chemosensors7020018
  14. P. Sreedev, V. Rakesh, N.S. Roshima, Optical characterization of ZnO thin films prepared by Chemical bath deposition method. *IOP Conf. Series: Materials Science and Engineering* **377**, 012086 (2018). doi:10.1088/1757-899X/377/1/012086
  15. S. Venkatachalam, Y. Iida, Y. Kanno, *Superlattices Microstruct.* **44**, 127 (2008). <https://doi.org/10.1016/j.spmi.2008.03.006>
  16. R.K. Jamal, M.A. Hameed, K.A. Adem, Optical properties of nanostructured ZnO prepared by a pulsed laser deposition technique. *Mater. Lett.* **132**, 31–33 (2014). <http://dx.doi.org/10.1016/j.matlet.2014.06.047>
  17. B. Sarma, D. Barman, B.K. Sarma, AZO (Al:ZnO) thin films with high figure of merit as stable indium free transparent conducting oxide[J]. *Appl. Surf. Sci.* **479**, 786–795 (2019) (JUN.15)
  18. T. Ohgaki, N. Ohashi, H. Kakemoto, S. Wada, Y. Adachi, H. Haneda, T. Tsurumi: *J. Appl. Phys.* **93** (2003) 1961. <https://doi.org/10.1063/1.1535256>
  19. H. Ahmoum, G. Li, S. Belakry, M. Boughrara, M.S. Su'ait, M. Kerouad, Q. Wang. “Structural, morphological and transport properties of Ni doped ZnO thin films deposited by thermal co-evaporation method”. *Materials Science in Semiconductor Processing*. Volume 123, 1 March 2021, 105530. <https://doi.org/10.1016/j.mssp.2020.105530>
  20. M. Purica, E. Budianu, E. Rusu, M. Danila, R. Gavrilă, *Thin Solid Films* **403–404**, 485 (2002). [https://doi.org/10.1016/S0040-6090\(01\)01544-9](https://doi.org/10.1016/S0040-6090(01)01544-9)

21. M. Harati, D. Love, W.M. Lau, Z. Ding, *Mater. Lett* **89**, 339 (2012)
22. V.G. Nair, R. Jayakrishnan, J. John, J.A. .Salam, A.M. Anand, A. Raj. "Anomalous photoconductivity in chemical spray pyrolysis deposited nano-crystalline ZnO thin films". *Materials Chemistry and Physics*, Volume 247, 1 June 2020, 122849. <https://doi.org/10.1016/j.matchemphys.2020.122849>
23. F. Yang, J. Song, X. Chen, X. Lu, J. Li, Q. Xue, B. Han, X. Meng, J. Li, Y. Wang, Ultrasonic spray pyrolysis-induced growth of highly transparent and conductive F, Cl, Al, and Ga co-doped ZnO films. *Sol. Energy* **228**, 168–174 (2021). <https://doi.org/10.1016/j.solener.2021.09.058>
24. S.K. Swami, N. Chaturvedi, A. Kumar, V. Kumar, A. Garg, V. Dutta, Spray deposited gallium doped zinc oxide (GZO) thin film as the electron transport layer in inverted organic solar cells ". *Sol. Energy* **231**, 458–463 (2022). <https://doi.org/10.1016/j.solener.2021.12.002>
25. A.F. Abdulrahman, S.M. Ahmed, N.M. Ahmed, M.A. Almessiere, Enhancement of ZnO nanorods properties using modified chemical bath deposition method: effect of precursor concentration. *Crystals* **10**(5), 386 (2020)
26. S. Shahzad, S. Javed, M. Usman, A review on synthesis and optoelectronic applications of nanostructured ZnO. *Front. Mater.* **8**, 613825 (2021). <https://doi.org/10.3389/fmats>
27. D. Krishnan, P. Sreedev, V. Rakhesh, N.S. Roshima, B. Shankar, S.M. Sunil. " Comparative Optical study of ZnO thin films prepared by SILAR Method". *AIP Conference Proceedings* **2162**, 020132 (2019); <https://doi.org/10.1063/1.5130342>
28. M. Carofiglio, S. Barui, V. Cauda, M. Laurenti, Doped zinc oxide nanoparticles: synthesis, characterization and potential use in nanomedicine. *Appl. Sci.* **10**(15), 5194 (2020)
29. J. Wojnarowicz, T. Chudoba, W. Lojkowski, A review of microwave synthesis of zinc oxide nanomaterials: reactants, process parameters and morphologies. *Nanomaterials* **10**(6), 1086 (2020)
30. Y. Natsume, H. Sakata, *Thin sol. films* **372**(1-2), 30 (2000)
31. O. Urper, O. Karacasu, H. Cimenoglu, N. Baydogan, Annealing ambient effect on electrical properties of ZnO:Al/p-Si heterojunctions. *Superlatt. Microstruct.* **125**, 81–87 (2019). <https://doi.org/10.1016/j.spmi.2018.10.027>
32. M. Nie, H. Sun, H.L. Cai, Z.H. Xue, C. Yang, Q. Li, L.Z. Qin, M.Y. Wu, *Mater. Lett.* **271**, 127785 (2020)
33. J. Mayandi, R.K. Madathil, C. Abinaya, K. Bethke, V. Venkatachalapathy, K. Rademann, T. Norby, T.G. Finstad, *Mater. Lett.* **288**, 129352 (2021)
34. D.B. Potter, M.J. Powell, I.P. Parkin, C.J. Carmalt, *J. Mater. Chem. C* **6**, 588–597 (2018)
35. J.N. Ma, W. Zhang, J.Y. Lin, Y. Sun, J.G. Ma, H.Y. Xu, Y.C. Liu, G.C. Yang. Theoretical study on group III elements and F co-doped ZnO. *J. Alloys Compd.* 819, (2020) 153012-1-153012-5
36. P. Dhamodharan, C. Manoharan, M. Bououdina, R. Venkadachalapathy, S. Ramalingam, Al-doped ZnO thin films grown onto ITO substrates as photoanode in dye sensitized solar cell. *Sol. Energy* **141**, 127–144 (2017). <http://dx.doi.org/10.1016/j.solener.2016.11.029>
37. C. Zegadi, A. Abderrahmane, A. Djelloul, S. Hamzaoui, M. Adnane, D. Chaumont, K. Abdelkebir, « Effects on structural and electro-optical properties of iron incorporation to p-zinc oxide (ZnO) thin

- films deposited by dip-coating process ». *Int. Rev. Phys.* 9 (2015)
38. M. Ayachi, F. Ayad, A. Djelloul, L. Benharrat, S. Anas. "Synthesis and Characterization of Ni-Doped ZnO Thin Films Prepared by Sol–Gel Spin Coating Method", *Semiconductors*, 2021, Vol. 55, No. 5, pp. 566–574. DOI: 10.1134/S1063782621050043
  39. A. Djelloul, Y. Larbah, M. Adnane, B. Labdelli, M.I. Ziane, A. Manseri, A. Messaoud, « Properties of Undoped and (Al, In) Doped ZnO Thin Films Prepared by Ultrasonic Spray Pyrolysis for Solar Cell Applications ». *J. Nano- Electron. Phys.* 10 No 2, 02036(5pp) (2018). DOI:10.21272/jnep.10(2).02036
  40. C.S. Prajapati, *P.P. Sahay*. « Influence of In doping on the structural, optical and acetone sensing properties of ZnO nanoparticulate thin films". *Materials Science in Semiconductor Processing* 16 (2013) 200–210. <http://dx.doi.org/10.1016/j.mssp.2012.04.015>
  41. F. Chouikh, Y. Beggah, M.S. Aida, "Physical Properties of Undoped and Doped ZnO Thin Films Prepared by Spray Pyrolysis for Photovoltaic Application ". *Int. J. Thin Fil. Sci. Tec.* **3**(2), 51–56 (2014). <http://dx.doi.org/10.12785/ijfst/030204>
  42. S. Ilıcan, M. Caglar, Y. Caglar, Sn Doping Effects on the Electro-Optical Properties of Sol Gel Derived Transparent ZnO Films. *Appl. Surf. Sci.* **256**, 7204–7210 (2010). <http://dx.doi.org/10.1016/j.apsusc.2010.05.052>
  43. A. Adjimi, M.L. Zeggar, N. Attaf, M.S. Aida, Fluorine-Doped Tin Oxide Thin Films Deposition by Sol-Gel Technique. *Journal of Crystallization Process and Technology* **8**, 89–106 (2018). <https://doi.org/10.4236/jcpt.2018.84006>
  44. A. Djelloul, M. Adnane, Y. Larbah, T. Sahraoui, C. Zegadi, A. Maha, B. Rahal, « Properties study of ZnS thin films prepared by spray pyrolysis method ». *J. Nano- Electron. Phys.* **7 No 4**, 04045 (2015)
  45. A. Mahroug, S. Boudjadar, S. Hamrit, L. Guerbous, Structural, optical and photocurrent properties of undoped and Al-doped ZnO thin films deposited by sol-gel spin coating technique. *Mater. Lett.* **134**, 248–251 (2014)
  46. Y. Caglar, M. Caglar, Microstructural IlıcanS. Optical and electrical studies on sol gel derived ZnO and ZnO:Al films. *Curr. Appl. Phys.* **12**, 963–968 (2012)
  47. J. Li, J. Xu, Q. Xu, G. Fang, Preparation and characterization of Al doped ZnO thin films by sol–gel process. *J. Alloys Compd.* **542**, 151–156 (2012)
  48. S. Ruzgar, M. Caglar, Fabrication and characterization of solution processed Al/Sn:ZnO/p-Si photodiodes. *Mater. Sci. Semicond.Process.* **115**, 105076 (2020). <https://doi.org/10.1016/j.mssp.2020.105076>
  49. H. Sutanto, S. Durri, S. Wibowo, H. Hadiyanto, E. Hidayanto, " Rootlike Morphology of ZnO: Al thin film deposited on amorphous glass substrate by Sol-Gel Method ". *Phys. Res. Int.* 2016, 4749587–4749597 (2016). <https://doi.org/10.1155/2016/4749587>
  50. S. Ilıcan, M. Caglar, Y. Caglar, Sn Doping Effects on the Electro-Optical Properties of Sol Gel Derived Transparent ZnO Films. *Appl. Surf. Sci.* **256**, 7204–7210 (2010). <http://dx.doi.org/10.1016/j.apsusc.2010.05.052>

51. A. Derbali, A. Attaf, H. Saidi, H. Benamra, M. Nouadji, M.S. Aida, N. Attaf, H. Ezzaouia, Investigation of structural, optical and electrical properties of ZnS thin films prepared by ultrasonic spray technique for photovoltaic applications. *Optik* **154**, 286–293 (2018).  
<https://doi.org/10.1016/j.ijleo.2017.10.034>
52. B. Subramanian, C. Sanjeeviraja, M. Jayachandran, *J. Crystal Growth* **234**, 421 (2002)
53. A. Djelloul, M. Adnane, Y. Larbah, M. Zerdali, C. Zegadi, A. Messaoud, « Effect of annealing on the properties of nanocrystalline CdS thin films prepared by CBD method ». *J. Nano- Electron. Phys.* **8**(No 2), 02005 (2016). DOI:10.21272/jnep.8(2).02005
54. A. Djelloul, M. Adnane, Y. Larbah, S. Hamzaoui, « Morphology, structural and optical study of ZnS thin films prepared by Successive Ionic Layer Adsorption and Reaction (SILAR) Method ». *J. Opt. Adv. Mater.* **18**(1-2), 136 (2016)
55. A. Herzi, M. Sebais, B. Boudine, O. Halimi, B. Rahal, L. Guerbous. " Fabrication and Characterization of Highly Textured Thin Films of Undoped and Ag-Doped ZnO ". *ACTA PHYSICA POLONICA A*, 135 (2019) 3. DOI:10.12693/APhysPolA.135.526
56. X.R. Deng, H. Deng, M. Wei, J.J. Chen, Preparation of highly transparent conductive Al-doped ZnO thin films and annealing effects on properties. *J Mater Sci Mater Electron* **23**, 413–417 (2012)
57. J. Li, J. Xu, Q. Xu, G. Fang, Preparation and characterization of Al doped ZnO thin films by sol–gel process. *J. Alloys Compd.* **542**, 151–156 (2012)
58. P.S. Xu, Y.M. Sun, C.S. Shi, Electronic structure of ZnO and its defects. *Sci China Ser A.* **44**, 1174–1181 (2001)
59. D. Behera, B.S. Acharya, Nano-star formation in Al-doped ZnO thin film deposited by dip-dry method and its characterization. *J. Lumin* **128**, 1577–1586 (2008)
60. J.J. Ding, H.X. Chen, S.Y. Ma, Structural and photoluminescence properties of Al-doped ZnO films deposited on Si substrate. *Physica E* **42**, 1861–1864 (2010)
61. T. Wang, Y. Liu, Q. Fang, M. Wu, X. Sun, F. Lu, Low temperature synthesis wide optical band gap Al and (Al,Na) co-doped ZnO thin films. *Appl Surf Sci* **257**, 2341–2345 (2011)
62. M.H. Mamat, M.Z. Sahdan, Z. Khusaimi, A.Z. Ahmed, S. Abdullah, M. Rusop. "Influence of doping concentrations on the aluminum doped zinc oxide thin films properties for ultraviolet photoconductive sensor applications", *Opt. Mater.* **32**, 696–699 (2010).  
doi:10.1016/j.optmat.2009.12.005

## Figures

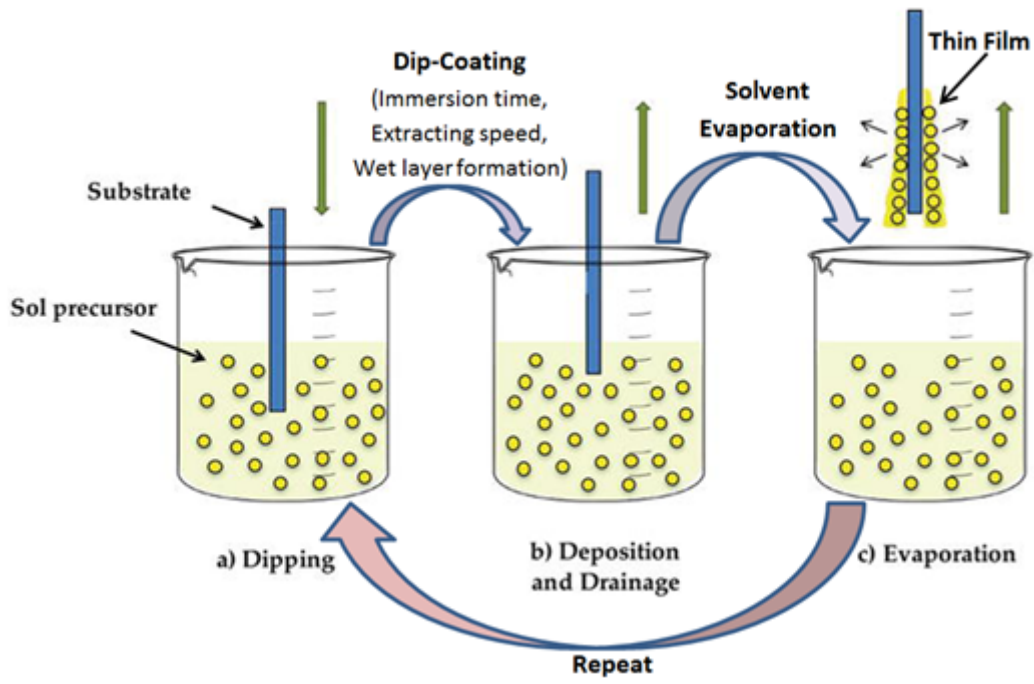


Figure 1

Stages of the sol-gel dip coating process.

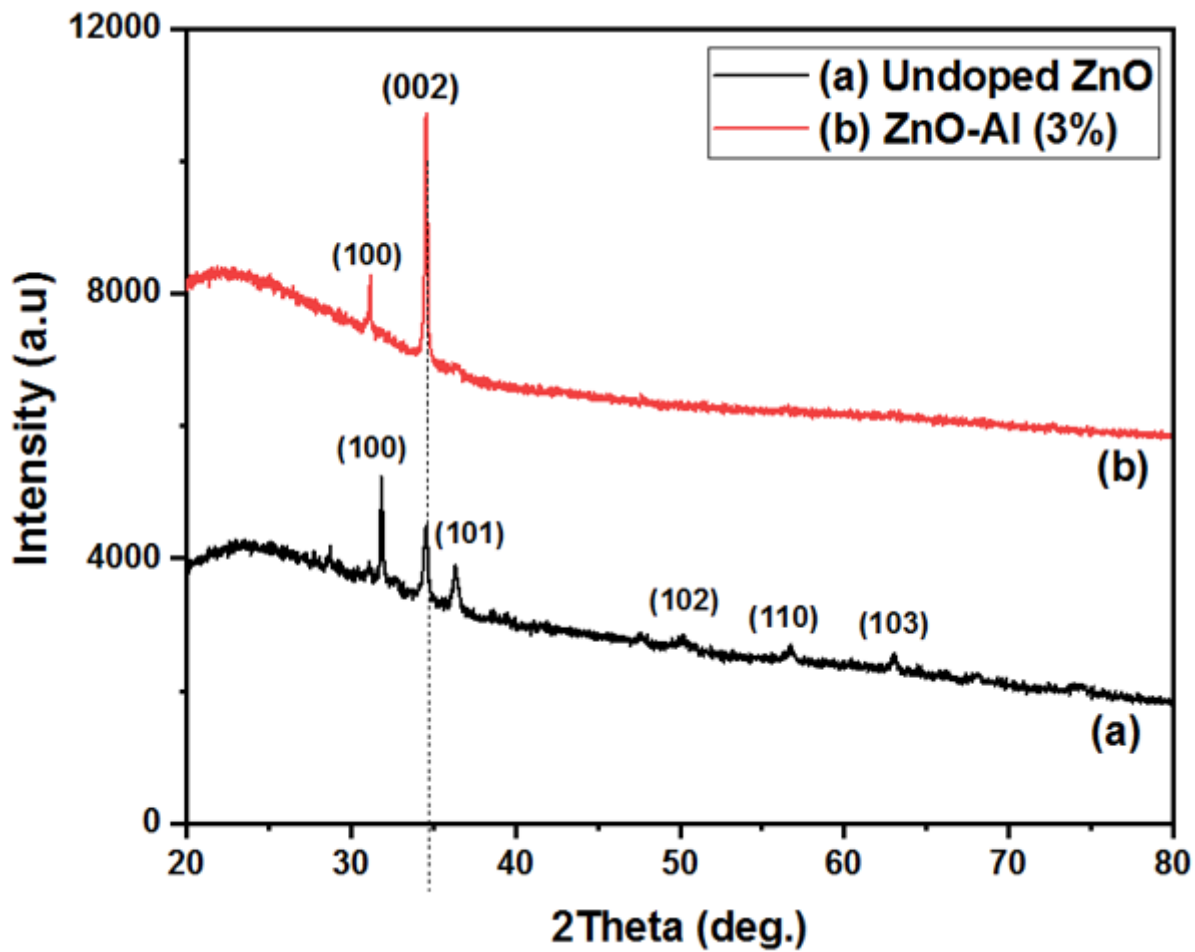


Figure 2

X-ray diffraction diffractograms of undoped and Al-doped ZnO (Al: 3 wt. %) semiconductor thin films.

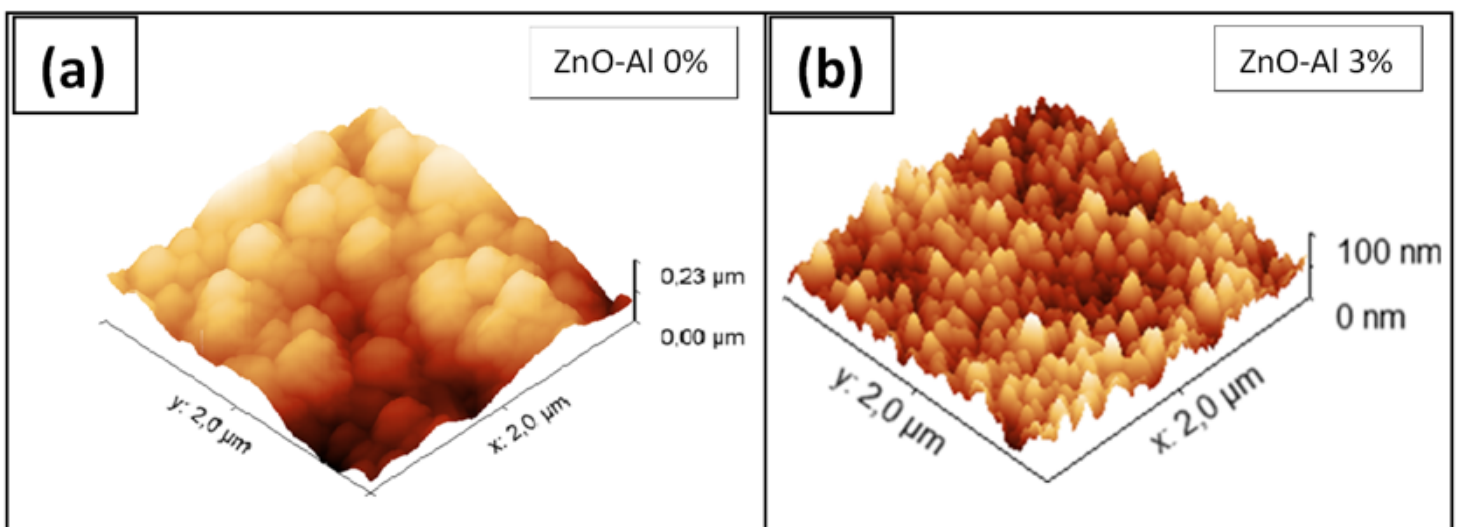
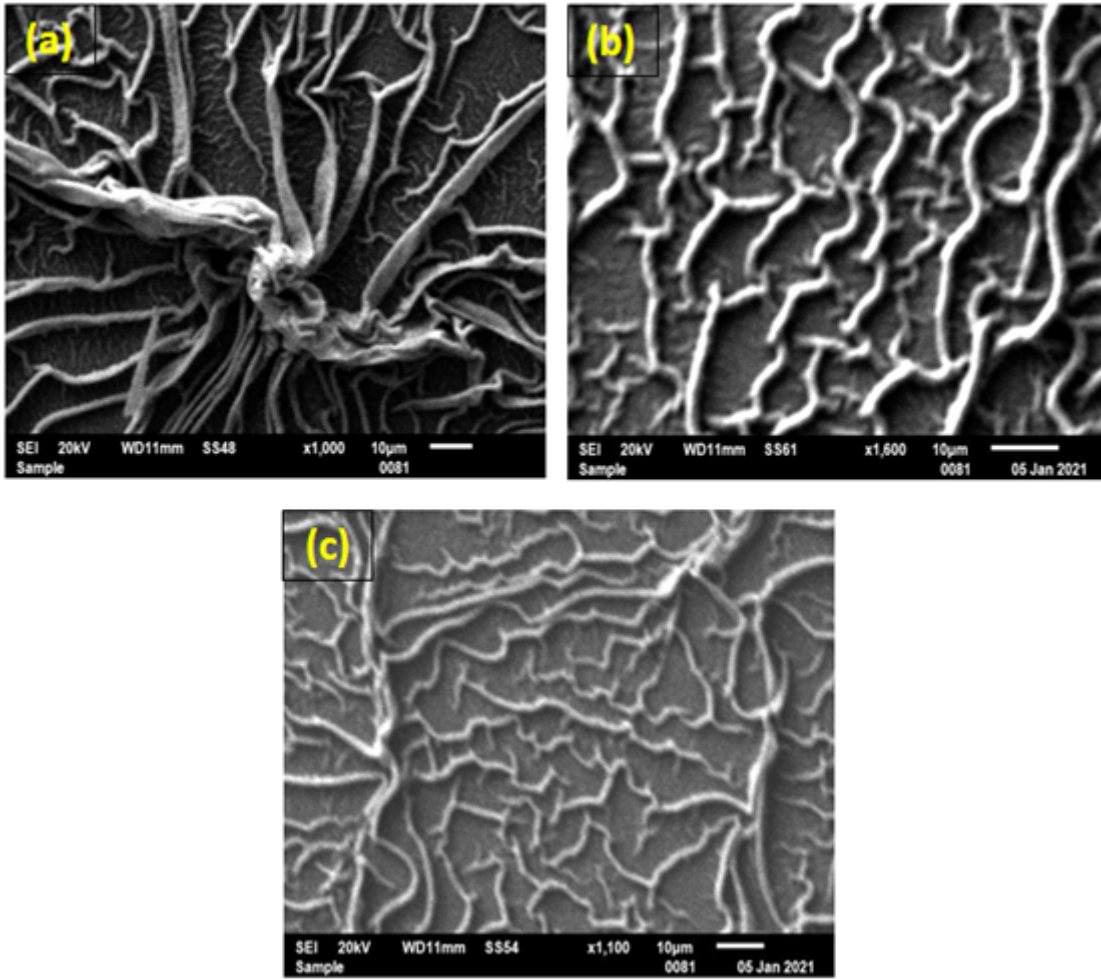


Figure 3

The 3D AFM images of (a) undoped ZnO ( $R_a=1.1$ ,  $R_q=1.3$ ) and (b) Al-doped ZnO (Al: 3 wt. %) ( $R_a=2.13$ ,  $R_q=2.68$ ) semiconductor thin films.



**Figure 4**

SEM images of: a) undoped ZnO, b) Al-doped ZnO (Al: 2 wt. %) and c) Al-doped ZnO (3 wt. %) semiconductor thin films.

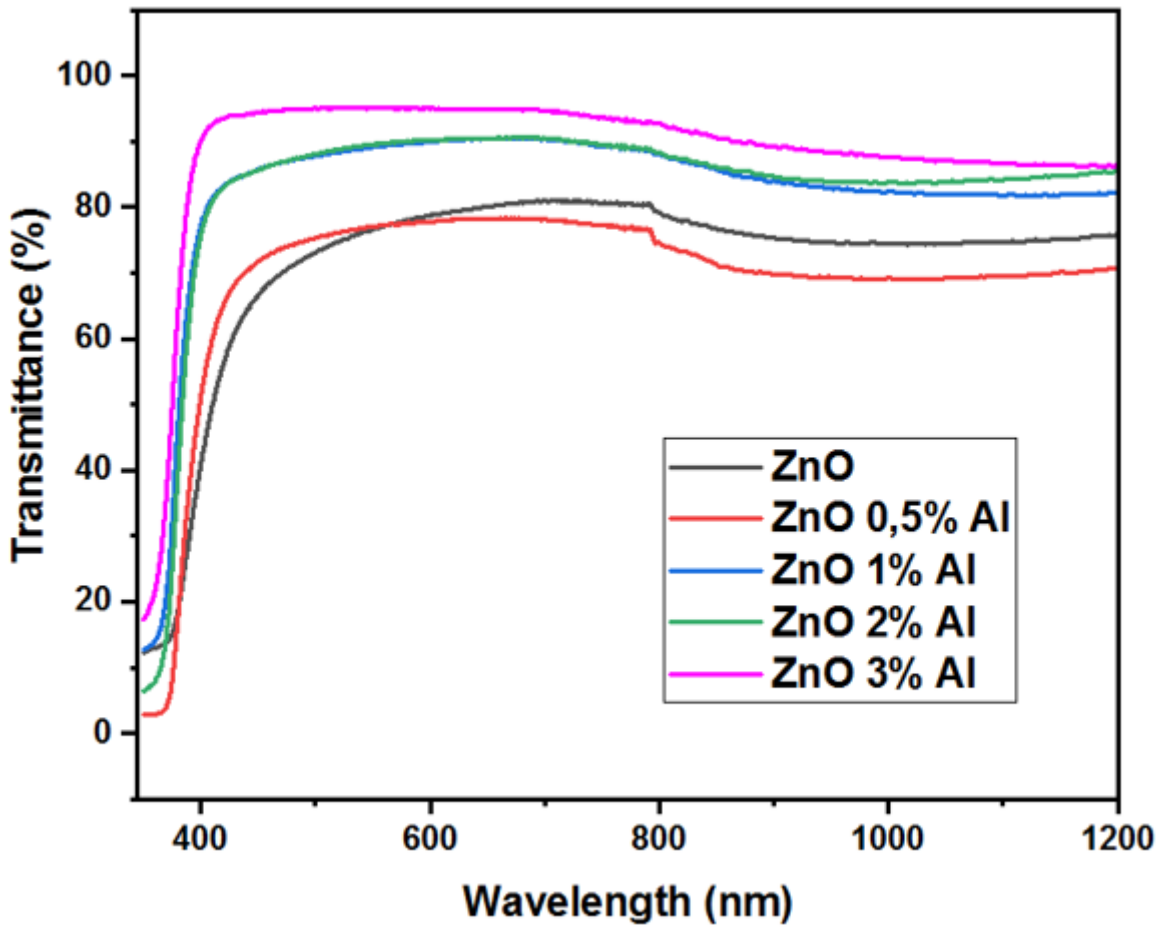


Figure 5

The optical transmittance spectra of undoped and Al-doped ZnO (Al: 0.5, 1, 2 and 3 wt. %) semiconductor thin films.



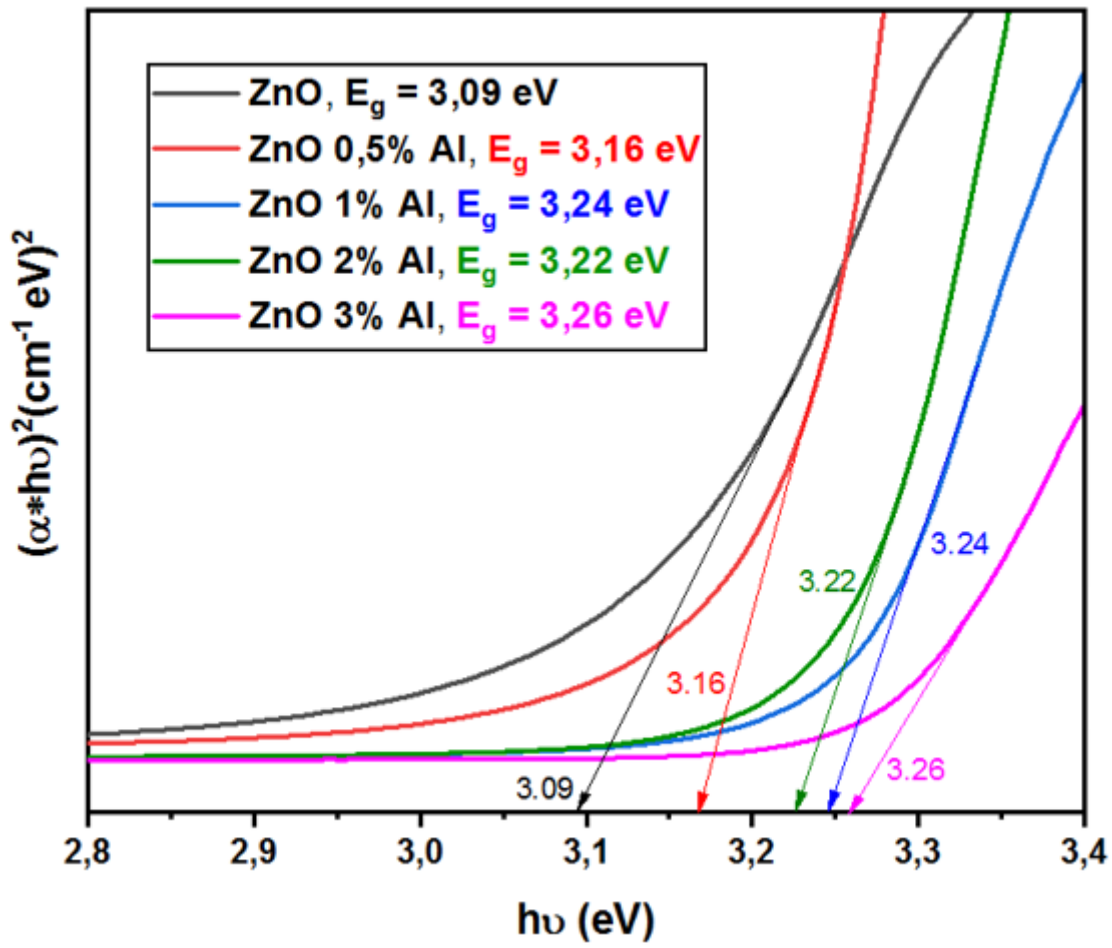


Figure 6

The Plot of  $(\alpha h\nu)^2$  versus  $h\nu$  of undoped and Al-doped ZnO (Al: 0.5, 1, 2 and 3 wt. %) semiconductor thin films.

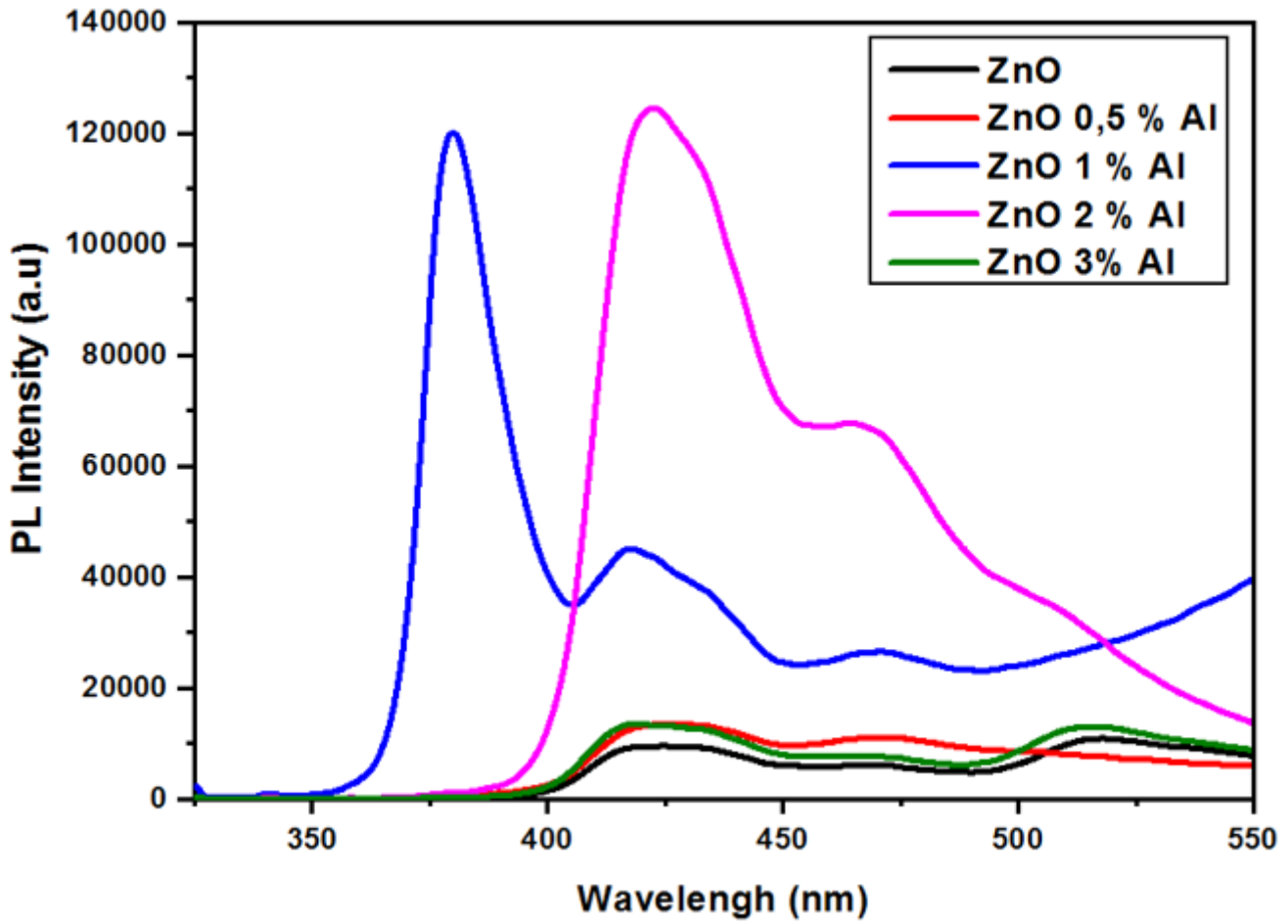


Figure 7

The photoluminescence spectra of undoped and Al-doped ZnO (Al: 0.5, 1, 2 and 3 wt. %) semiconductor thin films.

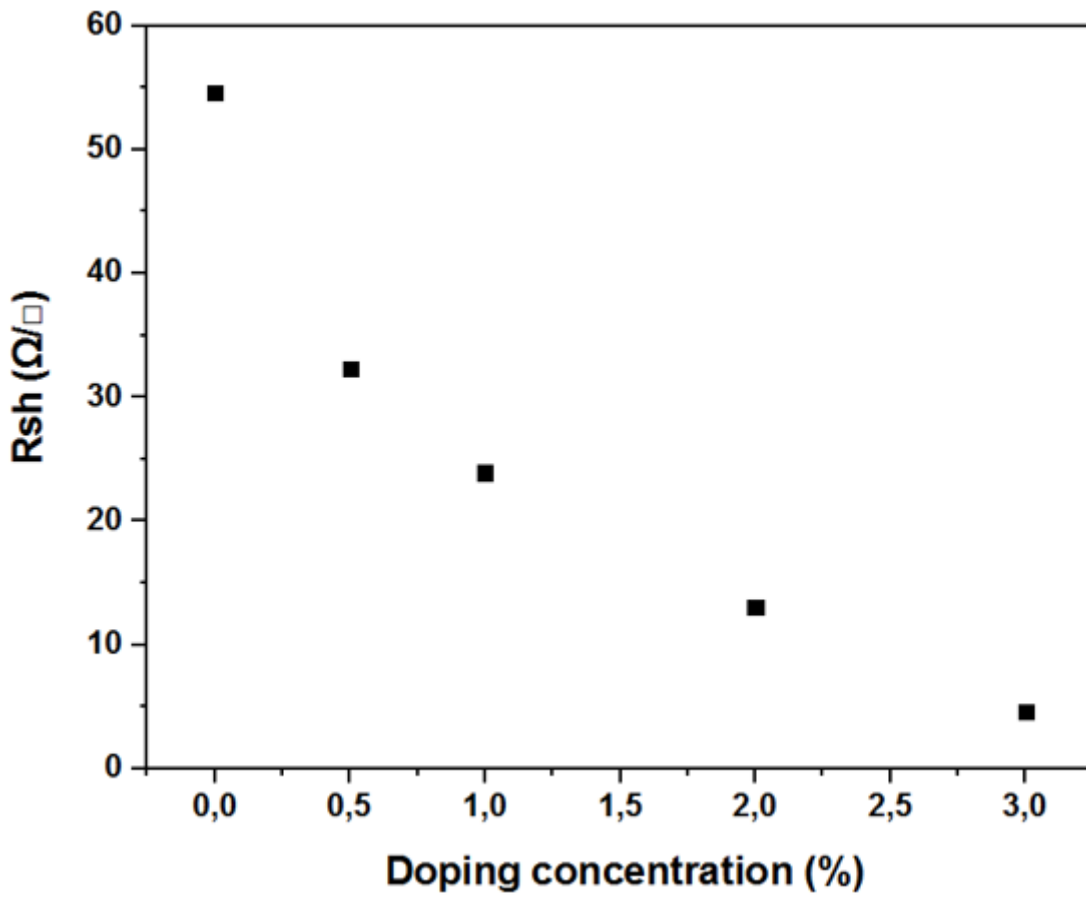


Figure 8

Sheet resistance of ZnO thin films as a function of different aluminium (Al) concentrations (Al: 0, 0.5, 1, 2, and 3 wt.%).